Article

Projected Aerosol Changes Driven by Emissions and Climate Change Using a Machine Learning Method

Huimin Li, Yang Yang,* Hailong Wang, Pinya Wang, Xu Yue, and Hong Liao

Read Online

ACCESS | Metrics & More | Article Recommendations | Supporting Information

ABSTRACT: Projection of future aerosols and understanding the driver of the aerosol changes are of great importance in improving the atmospheric environment and climate change mitigation. The latest Coupled Model Intercomparison Project Phase 6 (CMIP6) provides various climate projections but limited aerosol output. In this study, future near-surface aerosol concentrations from 2015 to 2100 are predicted based on a machine learning method. The machine learning model is trained with global atmospheric chemistry model results and projects aerosols with CMIP6 multi-model simulations, creatively estimating future aerosols with all important species considered. $PM_{2.5}$ (particulate matter less than 2.5 μm in diameter) concentrations in 2095 (2091−2100 mean) are projected to decrease by 40% in East Asia, 20−35% in South Asia, and 15−25% in Europe and North America, compared to those in 2020 (2015−2024 mean), under low-emission scenarios (SSP1-2.6 and SSP2-4.5), which are mainly due to the presumed emission reductions. Driven by the climate change alone, $PM_{2.5}$ concentrations would increase by 10−25% in northern China and western U.S. and decrease by 0−25% in southern China, South Asia, and Europe under the high forcing scenario (SSP5-8.5). A warmer climate exerts a stronger modulation on global aerosols. Climate-driven global future aerosol changes are found to be comparable to those contributed by changes in anthropogenic emissions over many regions of the world in high forcing scenarios, highlighting the importance of climate change in regulating future air quality.

KEYWORDS: *future aerosol concentrations, climate change, machine learning, anthropogenic emissions, GEOS-Chem, CMIP6*
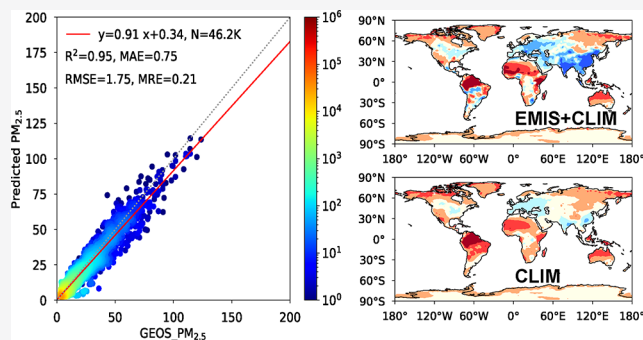
1. INTRODUCTION

Aerosols are one of the primary air pollutants that have adverse effects on the atmospheric environment and public health through damage to human respiratory and cardiovascular systems,[1] especially the particulate matter with a diameter of less than 2.5 μm ($PM_{2.5}$). Atmospheric aerosols impact regional and global climate in several ways.[2] Aerosols influence the Earth's radiation budget directly by absorbing and/or scattering solar radiation. On the other hand, aerosols modify the optical properties and lifetime of clouds and precipitation.[3,4] Therefore, a deeper understanding of atmospheric aerosols is of significance in both the environment and climate policy making.[5]

In recent decades, atmospheric aerosols have been changing considerably in various regions across the world. Since 1980s, aerosols have been decreasing in North America and Europe[6,7] but increasing in Asia until the implementation of clean air actions in China after 2013.[8−10] Monitoring networks, such as the Interagency Monitoring of Protected Visual Environments (IMPROVE)[11] in the United States and the European Monitoring and Evaluation Programme (EMEP)[12] in Europe, were established to measure near-surface aerosol concen-

trations. However, very few long-term monitoring networks exist in developing countries.[13] Numerical models have been widely applied to reproduce global aerosols in many previous studies to complement the limited observational data (e.g., Wang et al.[14]). Moreover, machine learning methods are useful in depicting the spatial distribution and temporal variations of atmospheric aerosols based on limited observations. Li et al.[15] constructed a gridded data set of near-surface $PM_{2.5}$ concentrations over China from 1980 to 2019 using a machine learning approach, which showed a good performance in reproducing historical $PM_{2.5}$ concentrations, with a coefficient of determination of 0.96 between model-predicted values and observations.

Projections of future changes in atmospheric aerosols facilitate environmental and climate predictions. Within the

Table 1. Summary of Data Sets Used in This Study

data set type	variable	description	spatial resolution	time period	data source
aerosol	BC	black carbon	2° × 2.5°	2005−2014 (historical)	GEOS-Chem simulation
	OC	organic carbon			
	NH_4^+	ammonium			
	NO_3^-	nitrate			
	SO_4^{2-}	sulfate			
meteorology	T_2m	air temperature at 2 m	2° × 2.5°	2005−2014 (historical); 2015−2100 (future)	MERRA-2 (historical); adjusted CMIP6 (future)
	T_850	air temperature at 850 hPa			
	T_500	air temperature at 500 hPa			
	U_850	zonal wind at 850 hPa			
	U_500	zonal wind at 500 hPa			
	V_850	meridional wind at 850 hPa			
	V_500	meridional wind at 500 hPa			
	RH	relative humidity			
	PRECP	precipitation rate			
	CLT	total cloud cover			
	RSDS	incoming shortwave radiation at the surface			
	SLP	sea level pressure			
emission	BC	black carbon	2° × 2.5°	2005−2014 (historical); 2015−2100 (future)	CMIP6 (global, historical and future); MEIC (China, historical)
	OC	organic carbon			
	CO_BB	carbon monoxide from biomass burning			
	CO_Anthro	carbon monoxide from anthropogenic sources			
	MTERP	monoterpenes		2014	
	ISOP	isoprene		2014	
	NH_3	ammonia		2005−2014 (historical); 2015−2100 (future)	
	NO_x	nitrogen oxides			
	SO_2	sulfur dioxide			
land use	LC	land cover	300 m × 300 m	2010	ESA CCI
	NDVI	normalized difference vegetation index	0.05° × 0.05°	2010	AVHRR
topography	TOPO	digital elevation model	90 m × 90 m	2010	SRTM

latest Coupled Model Intercomparison Project Phase 6 (CMIP6),[16] the Scenario Model Intercomparison Project (ScenarioMIP)[17] provides future projections of many climate variables based on state-of-the-art climate models with various emission scenarios and land use changes under the Shared Socioeconomic Pathways (SSPs). However, many of the CMIP6 models do not provide variables of aerosol components and chemical processes since they focus on future changes in climate rather than air quality.[18,19] Moreover, different aerosol components, such as nitrate, ammonium, and organic aerosols, are not fully represented in the majority of climate models, partly due to the consideration of the computational efficiency.[20,21] With available data, Turnock et al.[20] reported that $PM_{2.5}$ was underrepresented in the CMIP6 models over Asia, Europe, and North America. Some studies directly used emissions in the future scenarios as input to global chemical transport models, driven by present-day meteorological data, to project future aerosol changes.[22,23] This method does not take into account any impacts of climate change on aerosols through chemical, transport, and scavenging processes.

In addition to anthropogenic emissions, changes in meteorological fields under climate change may also exert significant influences on aerosol concentrations.[24−26] Cai et al.[25] found that in a high forcing scenario, the frequency of weather conditions conducive to severe haze events in northern China would increase by 50% in 2050−2099 relative

to 1950−1999 due to the strengthened atmospheric stagnation under global warming. Gonzalez-Abraham et al.[27] and Val Martin et al.[28] projected increases in $PM_{2.5}$ concentrations in many U.S. regions as a result of increases in biogenic emissions, land use changes, and wildfire burning related to the meteorological changes. However, it is also argued that there would be a negligible change in extreme winter haze events in northern China[29] and a decrease in $PM_{2.5}$ concentrations in the U.S. due to increased precipitation in winter.[30] Effects of climate change on aerosols are complicated because projections of the dominant meteorological factors driving aerosol variations are often unreliable.[31] Nonetheless, many of the findings mentioned above are based on regional downscaling simulations with meteorological factors coming from one single climate model, which have large uncertainties in the future aerosol prediction.

In this study, global near-surface aerosol concentrations during 2015−2100 are projected using a combination of data sets, including speciated present-day global three-dimensional aerosols from an atmospheric chemical transport model (GEOS-Chem), SSP future emissions, meteorological fields from CMIP6 multi-model simulations, and other auxiliary data, together with a machine learning method. The impact of climate change on aerosol concentrations is also quantitatively separated out from that driven by both emissions and climate change. The novel method in this study takes advantage of the chemical transport model in predicting more complete aerosol
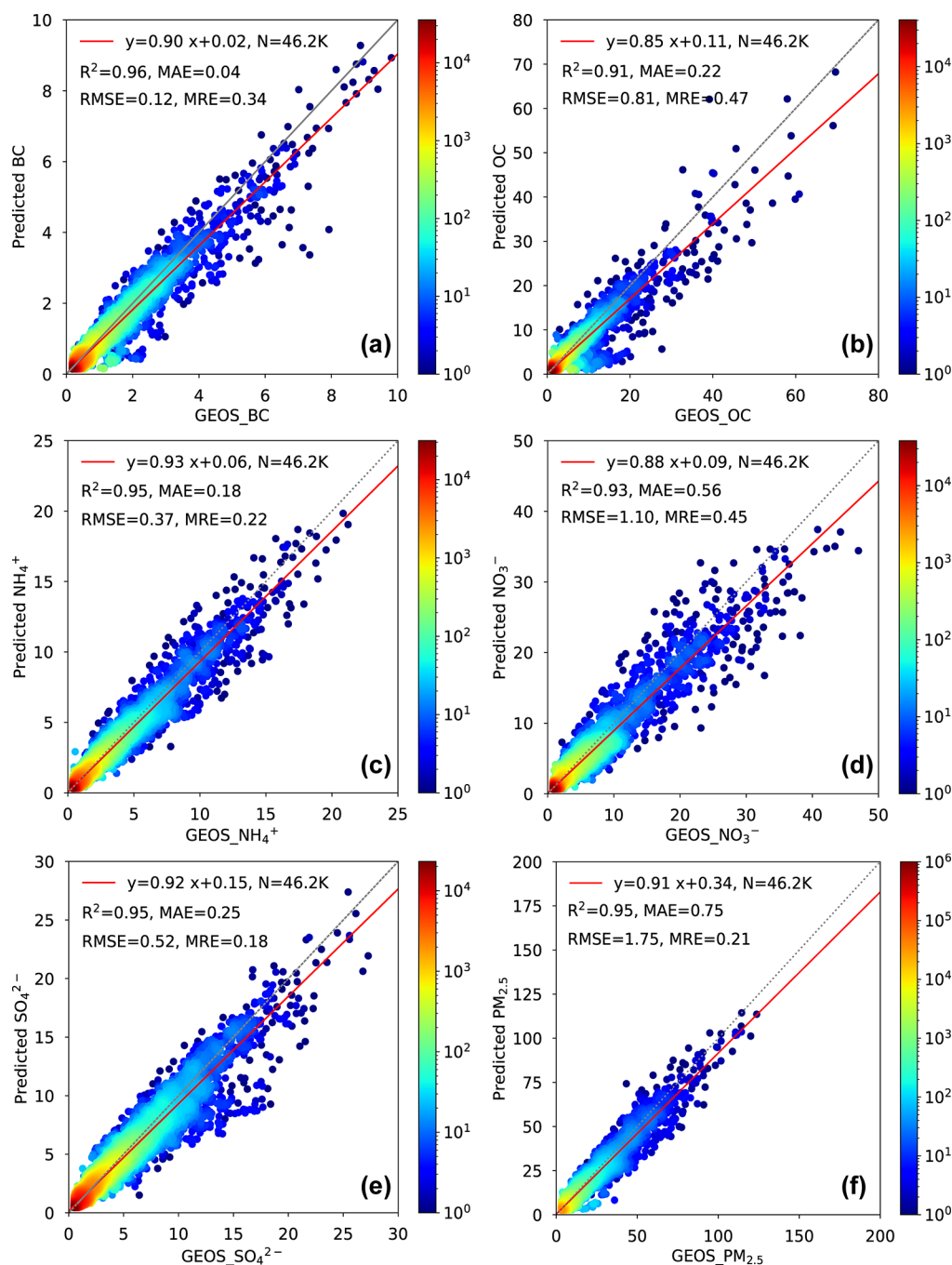
Figure 1. Density scatterplots of predicted vs simulated near-surface aerosol concentrations (BC, OC, NH4$^+$, NO$_3^-$, SO$_4^{2-}$, and PM$_{2.5}$, μg m^{-3}) using the testing samples in 2010. The gray and red solid lines show the 1:1 line and linear regression line, respectively. Statistical metrics including R^2 (unitless), RMSE (μg m^{-3}), MAE (μg m^{-3}), and MRE (%) are given at the top left of each panel. The PM$_{2.5}$ concentration is calculated as the sum of concentrations of BC, OC, NH4$^+$, NO$_3^-$, and SO$_4^{2-}$ in this study.

species with future climate from multi-models, with the consideration of the impact from climate change on aerosols.

2. MATERIALS AND METHODS

2.1. GEOS-Chem Model Simulations. To train the machine learning model, historical aerosol concentrations are required and are produced by a global chemical transport model simulation. In this study, 10 year global speciated aerosols, including black carbon (BC), organic carbon (OC, sum of primary and secondary organic carbon), ammonium (NH$_4^+$), nitrate (NO$_3^-$), and sulfate (SO$_4^{2-}$), over 2005−2014

are produced by the GEOS-Chem model v12.9.3 (http://acmg.seas.harvard.edu/geos/), which is driven by the Modern-Era Retrospective analysis for Research and Applications, version 2 (MERRA-2) meteorological fields.[32] The GEOS-Chem model here employs 47 vertical levels and a horizontal resolution of 2° latitude by 2.5° longitude. It has fully coupled aerosol−O$_3$−NO$_x$−hydrocarbon chemical representations.[33−35] The PM$_{2.5}$ concentration is calculated as the sum of concentrations of BC, OC, NH$_4^+$, NO$_3^-$, and SO$_4^{2-}$ in this study. The secondary organic aerosol (SOA) in OC is simulated using the simple SOA scheme, which requires
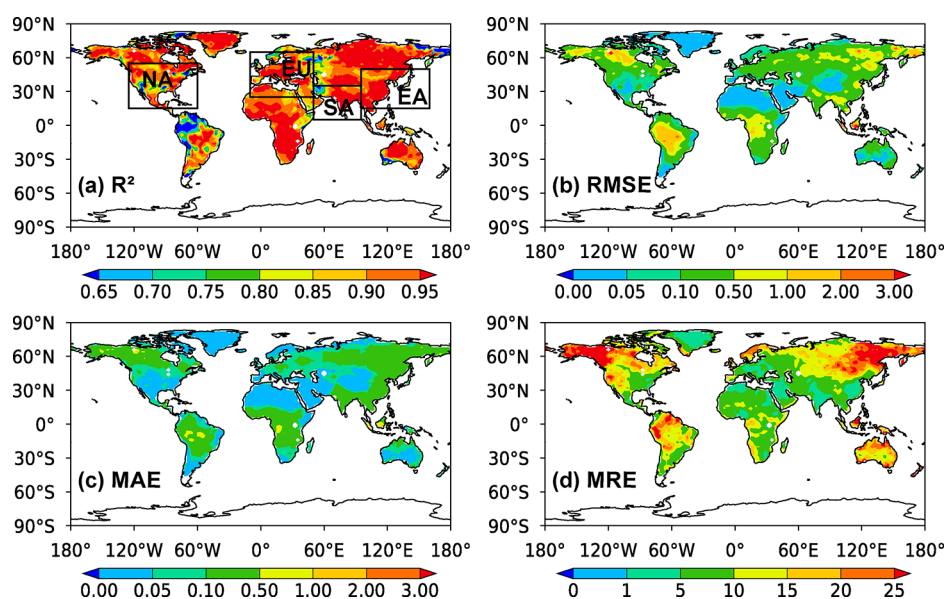
Figure 2. Spatial distributions of the performance statistics of the RF model-estimated historical PM$_{2.5}$ concentrations in regards to (a) R^2 (unitless), (b) RMSE (μg m^{-3}), (c) MAE (μg m^{-3}), and (d) MRE (%) over 2005−2014. The box-outlined areas in (a) mark East Asia (EA, 15−50°N, 95−160°E), Europe (EU, 25−65°N, 10°W−50°E), North America (NA, 15−55°N, 60−125°W), and South Asia (SA, 5−35°N, 50−95°E).

emissions of monoterpenes, isoprene, and anthropogenic and biomass burning carbon monoxide (CO). The GEOS-Chem model has proven to be a practical tool in simulating atmospheric compositions and spatiotemporal distributions of aerosols on local to global scales.[36−38] We perform a GEOS-Chem simulation from 2005 to 2014 using both emissions and meteorological fields varying with time during the simulation.

The global historical (2005−2014) monthly anthropogenic and biomass burning emissions of aerosols and their precursors are obtained from the CMIP6 experiment.[39,40] During the recent decades, anthropogenic emissions of aerosols have changed greatly since the implementation of clean air actions over China.[15,41] The Multi-resolution Emissions Inventory (MEIC), which is a national emission inventory for China, instead of CMIP6 is used for anthropogenic aerosol emissions over China. Furthermore, as the machine learning input data, we interpolate the decadal emissions over 2015−2100 under SSPs from CMIP6 into each year using the linear interpolation method. In general, emissions of BC, OC, NO$_x$, and SO$_2$ are projected to decrease in the future, while the NH$_3$ emission has no significant trend (Figure S1). There is a discontinuity in emissions between 2014 (historical) and 2015 (future) because MEIC emissions are used to replace the CMIP6 historical emissions in China. The overestimate of anthropogenic emissions in 2015 could cause an overestimate of future aerosol concentrations. SSP scenarios that do not fully consider regional pollution control policies would also overestimate the impact of climate change on aerosols.

2.2. CMIP6 Multi-Model Simulations. Predicting future aerosol concentrations using a trained machine learning model needs meteorological field data under future scenarios, which can be obtained from the ScenarioMIP multi-model simulations in CMIP6 (https://esgf-node.llnl.gov/search/cmip6/). In this study, a variety of monthly meteorological variables, including air temperatures at 2 m, 850 hPa, and 500 hPa, wind fields at 850 and 500 hPa, precipitation rate, total cloud cover, relative humidity, sea level pressure, and incoming shortwave radiation at the surface, are selected to predict aerosol concentrations (Table 1). These meteorological factors have shown substantial influences on aerosols.[25,42−50]

In total, 18 CMIP6 models (ACCESS-CM2, ACCESS-ESM1-5, CanESM5, CESM2-WACCM, CMCC-CM2-SR5, EC-Earth3-Veg, EC-Earth3, FGOALS-f3-L, FGOALS-g3, GFDL-ESM4, INM-CM5-0, IPSL-CM6A-LR, MIROC6, MPI-ESM1-2-HR, MPI-ESM1-2-LR, MRI-ESM2-0, Nor-ESM2-LM, and NorESM2-MM) have all of these monthly meteorological fields under four future scenarios, including the sustainable scenario (SSP1-2.6), medium forcing scenario (SSP2-4.5), medium to high forcing scenario (SSP3-7.0), and high forcing scenario (SSP5-8.5). Note that our machine learning model is trained with GEOS-Chem meteorological fields originally obtained from MERRA-2 reanalysis but predicts aerosols with CMIP6 model-simulated meteorology under climate change. To minimize the impact of inconsistency in meteorology between CMIP6 models and the GEOS-Chem model, the CMIP6 meteorological variables in 2015−2100 are adjusted by their potential bias, characterized as the difference in their historical climatological mean (2005−2014) and MERRA-2. This adjustment process also removes inconsistency in the initial conditions of meteorological fields used by different CMIP6 models.

2.3. Predicting Aerosols Using a Machine Learning Method. Machine learning has been widely adopted in recent aerosol studies because of its computational efficiency and superior performance.[15,51,52] Here, we use a random forest (RF) model to predict global aerosol concentrations with input data of GEOS-Chem aerosol concentrations, meteorological parameters, emissions, land cover (LC, http://maps.elie.ucl.ac.be/CCI/viewer/download.php), topography (TOPO, https://cgiarcsi.community/data/srtm-90m-digital-elevation-database-v4-1/), normalized difference vegetation index (NDVI, https://www.ncei.noaa.gov/data/avhrr-land-normalized-difference-vegetation-index/access/), and spatiotemporal information (month of the year and geographic location of each model grid), following Li et al.[15] The RF model is individually trained and then predicts concentrations for each aerosol
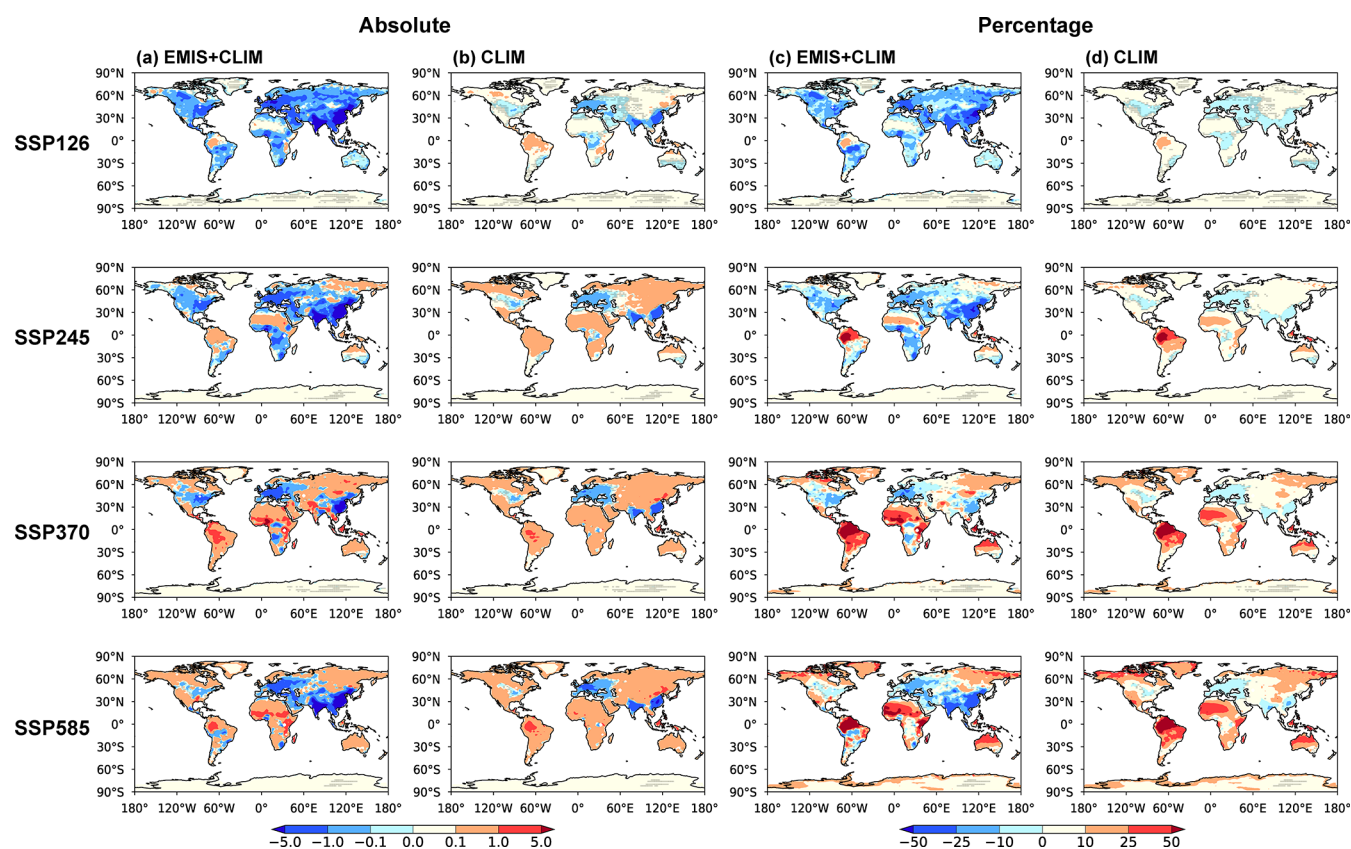
Figure 3. Spatial distributions of differences $(\mu g\ m^{-3})$ in future global near-surface $PM_{2.5}$ concentrations under the four scenarios (SSP1-2.6, SSP2-4.5, SSP3-7.0, and SSP5-8.5, from the top to the bottom) between 2020 (2015−2024 mean) and 2095 (2091−2100 mean) with both emissions and meteorological fields changed (a), and only meteorological fields changed (b), respectively. Right two columns show percentage differences (%) in 2095 (2091−2100 mean) relative to 2020 (2015−2024 mean) with both emissions and meteorological fields changed (c) and only meteorological fields changed (d). No overlay indicates statistical significance with 95% confidence from a two-tailed t test.

component. Steps showing the concrete procedure of using the RF model for predicting future near-surface aerosol concentrations are presented in Text S1. Although the machine learning model testing is based on the data sets in 2010, which is the warmest year over land during 2005−2014, the air temperature will also be higher under the influence of greenhouse gases in the future scenarios.

3. RESULTS

3.1. RF Model Performance in Aerosol Prediction. The RF model performance in predicting aerosol components and $PM_{2.5}$ concentrations across the globe in 2010 is characterized with aerosol data samples from GEOS-Chem and is shown in Figure 1. The predictive capability of the RF model is crucial for determining whether it can predict aerosols in the future well. The predicted $PM_{2.5}$ concentrations manifest a good consistency with the corresponding GEOS-Chem simulations in 2010, with an R^2 of 0.95 and a magnitude of relative error (MRE) of 21%, demonstrating a good performance of the RF model. By examining the importance scores, referred to as the scores of input features in predicting aerosols, emission is found to be the most important feature for the RF model with individual contributions of 30−60% for different aerosol species, and emission is also strongly correlated with aerosol concentrations with a correlation coefficient (R) of 0.6−0.9 (Figure S2). Land cover contributes 10% to the model and is negatively correlated with aerosol concentrations. Other factors have individual contributions less than 10%. Temper-

ature at 2 m and sea level pressure are positively correlated with many aerosol concentrations with an R higher than 0.5.

Figure 2 presents the spatial distributions of statistical metrics for the RF model in estimating near-surface $PM_{2.5}$ concentrations during 2005−2014. Overall, the RF model performs well with small estimation biases in most areas of the globe. Approximately 80% of land areas have an R^2 greater than 0.85, particularly in the key regions of interest including East Asia, South Asia, Europe, and North America. Around 85% (99%) of land areas have low estimation biases with a root mean squared error (RMSE) [mean absolute error (MAE)] < 0.5 $\mu g/m^3$. Moreover, 91% of land areas have an MRE of less than 25%. Note that the model has a relatively large bias in estimating aerosols over high-latitude North America and Asia, which are mostly related to the pollutant transport from mid-latitudes or the local burning emissions,[53,54] suggesting that the model can be improved by taking these factors, such as wind fields over the source regions, into consideration in the future studies. Similar statistical metrics for individual aerosol components are given in Figure S3.

The RF model performance in the temporal variation of $PM_{2.5}$ estimation from 2005 to 2014 is evaluated and presented in Figure S4. The RF model-estimated global $PM_{2.5}$ concentration is highly correlated with the GEOS-Chem simulation with above 93% of the days having an $R^2 > 0.95$. More than 96% of the days have an RMSE (MAE) lower than 1.0 (0.3) $\mu g/m^3$, and 93% of the days have an MRE lower than 25%. This does show that biases increase in boreal summer
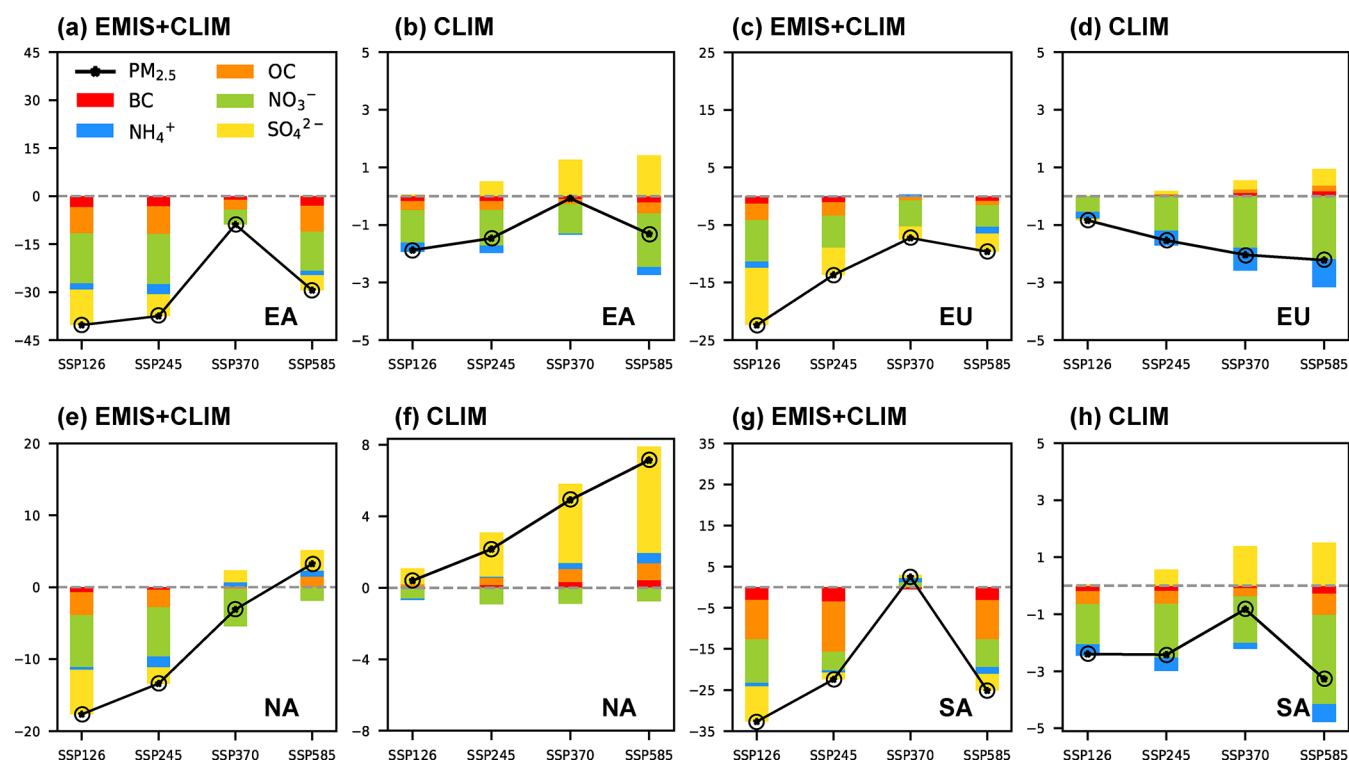
Figure 4. Percentage change (%) of near-surface aerosol concentrations (BC, OC, NH4+, NO$_3^-$, SO$_4^{2-}$, and PM$_{2.5}$) under the four SSP scenarios in 2095 relative to 2020 with both emissions and meteorological fields changed and only meteorological fields changed, respectively, over four selected regions including EA (a,b), EU (c,d), NA (e,f), and SA (g,h). Circles denote that the changes are statistically significant at the 95% confidence level from a two-tailed Student's t test.

and decrease in boreal winter mostly due to the OC estimation (Figure S5). In general, these statistical metrics indicate that the RF model is capable of describing the spatial distributions and temporal variations of near-surface aerosol concentrations in many regions of the globe.

3.2. Projection of Aerosol Variations in the Future. Figure 3a shows the spatial differences in annual mean near-surface PM$_{2.5}$ concentrations between the first and last decade of 2015−2100 under the four scenarios with both varying emissions and meteorological fields, and Figure 3c gives the corresponding percentage values [concentrations in 2020 (2015−2024 mean) and 2095 (2091−2100 mean) are shown in Figure S6]. Concentrations of PM$_{2.5}$ and individual aerosol species (Figures S7−S11) are projected to decrease in 2095 compared to that in 2020 over many key regions of the world, including East Asia, South Asia, Europe, and North America in all SSPs, which is mostly related to the decreasing emissions in the future (Figure S12). The maximum decrease occurs in eastern China with a percentage decrease larger than 50% in SSP1-2.6 and SSP2-4.5 scenarios. Low emission scenarios (SSP1-2.6 and SSP2-4.5) produce a larger decrease in PM$_{2.5}$ concentrations than high forcing scenarios (SSP3-7.0 and SSP5-8.5), suggesting that sustainable development scenarios are the more favorable future paths in improving global air quality than high forcing scenarios. Over north of 60°N, PM$_{2.5}$ concentrations increase in all SSPs except SSP1-2.6, which is probably related to the RF model biases in predicting aerosols at high latitudes.

The percentage and absolute changes in regional aerosol concentrations between 2020 and 2095 under the four SSPs are shown in Figures 4 and S25, respectively. Over East Asia, the PM$_{2.5}$ concentrations is projected to decrease considerably

under the four future scenarios, with a maximum decrease of around 40% under the SSP1-2.6 and SSP2-4.5 scenarios. NO$_3^-$, OC, and SO$_4^{2-}$ decrease the most among all aerosol species, which primarily results from large reductions in future precursor emissions (Figure S12). Averaged over Europe and North America, the PM$_{2.5}$ concentrations would be reduced by 15−25% under low emission scenarios. It is interesting that concentrations of OC, SO$_4^{2-}$, and NH$_4^+$ would increase under SSP5-8.5 in North America (Figure 4e), although the aerosol and precursor emissions decrease in the future (Figure S1), indicating that climate change plays an important role in future aerosol changes over North America. PM$_{2.5}$ concentrations in South Asia are projected to decrease in all SSPs by 20−35%, except for SSP3-7.0 with a weak increase of less than 5% due to insignificant emission changes over this region.

3.3. Climate-Driven Aerosol Variations. In addition to changes in anthropogenic emissions, future aerosols can also be modulated by climate change. Figure 3b,d shows the absolute and percentage changes, respectively, in near-surface PM$_{2.5}$ concentrations in 2095 relative to 2020, driven by climate change associated with the four SSPs. Generally speaking, a warmer climate exerts a stronger modulation on global aerosols. The effects of climate change on the future aerosol changes are comparable to those driven by both anthropogenic emissions and climate change over many regions of the world in SSP5-8.5, highlighting the importance of climate change in the future aerosol variations. However, the PM$_{2.5}$ concentrations over East Asia, South Asia, and Europe would decrease by up to 25% driven by climate change alone, which are less than that due to both anthropogenic emissions and climate change (up to 50%) under the SSP5-8.5 scenario.

In China, aerosol changes show a dipole spatial pattern with increases in concentrations over northern China and decreases over southern China. By defining a haze weather index using CMIP5 data, Cai et al.[25] found that wintertime severe haze events would occur more frequently in Beijing over northern China under future climate change than that in historical conditions, while a negligible change was reported in another study.[29] Using the predicted aerosol concentrations with CMIP6 data, we show that the climate-driven $PM_{2.5}$ concentrations will increase by 10−25% in northern China under the high forcing scenarios in all seasons except spring (Figures S26−S29), supporting the finding of Cai et al.[25] Over South Asia and Europe, $PM_{2.5}$ concentrations are projected to decrease by up to 0−25% under the SSP5-8.5 climate change. $PM_{2.5}$ concentrations would increase by 10−25% in western U.S., which is mainly due to the increase in surface air temperature and decrease in precipitation over this region under the SSP5-8.5 scenario (Figure S30).

Averaged over East Asia, due to the offset of the dipole changes in northern and southern China, climate-driven annual $PM_{2.5}$ concentrations have small decreases (less than 3%) in 2095 relative to 2020 under all SSPs (Figure 4b). Future trends in meteorological parameters under climate change (Figures S13−S24) are responsible for the aerosol changes. SO_4^{2-} is projected to increase in East Asia under climate change and other aerosols will decrease, indicating that chemical production will increase in the warming climate but dynamical processes tend to reduce near-surface aerosols. The hypothesis can be confirmed by the increasing temperature (Figures S13−S15) over East Asia since higher temperature increases gas-phase reaction rates and oxidant concentrations.[55] As SO_4^{2-} increases, NO_3^- decreases because it competes with SO_4^{2-} for the available NH_3 to form ammonium nitrate. Also, increased precipitation in the warming climate will increase the wet scavenging efficiency of aerosols, leading to the decreases in aerosol concentrations. In addition to increases in SO_4^{2-}, OC also increases in Europe and North America, which offsets the decreases in other aerosols. The increases in OC are related to the decreases in relative humidity over Europe and North America in the future (Figure S20), considering that the concentration of SOA is negatively correlated with relative humidity,[56] which is also confirmed by the significant negative correlation between OC and relative humidity in Figure S2. Over South Asia, climate change will decrease $PM_{2.5}$ concentrations by 2−5%, associated with the increasing precipitation. All of the future regional aerosol variances controlled by the climate change are statistically significant at the 95% confidence level, except for East Asia under the SSP3-7.0 scenario.

4. DISCUSSION

Global near-surface aerosol concentrations during 2015−2100 are projected in this study based on a machine learning approach with input data from a GEOS-Chem simulation, CMIP6 multi-model simulations, and many other auxiliary data sets. Impacts from future emission change and climate change on aerosol variations are analyzed. We found that the impact of climate change on the future aerosol changes can be comparable to those driven by changes in anthropogenic emissions over many regions of the world in the high forcing scenario, and a warmer climate exerts a stronger modulation on global aerosols. This study highlights the importance of climate change in regulating future aerosol variations.

The $PM_{2.5}$ projections in this study over different regions of the world under future emission scenarios have been compared with many previous studies,[20,57−59] which are shown in Text S2 and Table S1. In this study, we use global emissions data sets for SSP scenarios to predict future aerosol variations. Considering that the CMIP6 future climate changes are also projected using the SSP emissions, it is desirable and appropriate to use the same emissions data sets for aerosols, along with other forcing agents, that drive the climate change under each scenario. However, we also note that individual countries or regions could have more reasonable and adaptive emission projections that take regional climate and clean air policies into account. As shown in Text S2, there are large discrepancies in regional results for China because SSPs do not consider the clean air policies and recent air quality improvements in China, leading to biased local emission estimates in China under SSPs and potential biases in the machine learning method. In future studies, localized emission data sets are more desirable in order to better project future air quality over specific regions.

In addition, the spatial differences in annual mean near-surface $PM_{2.5}$ concentrations between the first and last decade of 2015−2100 from one CMIP6 model (GFDL-ESM4) and the machine learning method driven by the GFDL-ESM4-predicted future meteorological parameters are similar to each other in many regions of the globe (Figure S31), except for high-latitude and desert regions, where the poor agreement likely results from the biased prediction of secondary aerosols (Figure S3), further confirming the good ability of the machine learning method to predict future aerosols.

Many countries have announced to achieve carbon neutrality by the middle of this century, which is an economy with net-zero greenhouse gas emissions. SSP1-1.9 is the most optimistic scenario representing carbon neutrality under CMIP6, but it is within Tier 2 of the ScenarioMIP framework.[17] The SSP1-2.6 scenario has a similar emission pathway to that of SSP1-1.9 and can be partly used to represent the carbon neutrality. Noted that, the pollutant emissions in 2050 under the SSP1-1.9 are lower than that of SSP1-2.6, indicating that aerosol concentrations would decrease faster in the first half of the 21st century under SSP1-1.9 than that under SSP1-2.6.

Note that there are a number of uncertainties in the prediction of future near-surface aerosol concentrations over the world, which could be due to the input data, GEOS-chem model, climate models, and the machine learning model. First of all, land use and topography data are fixed at the present-day conditions during the model prediction, which can also vary under future climate change. Furthermore, the inconsistency in CMIP6 emissions over China with the historical MEIC emission inventory could introduce additional biases to future aerosol predictions. In addition to the effects of climate change on aerosols, aerosols also have an impact on climate in multiple and complex ways through their interactions with radiation and clouds. Also, we did not consider potential future changes in fire and biogenic emissions and wind-blown dust in this study, which could vary under the projected climate change.[60,61]

Second, the training of the machine learning model uses the GEOS-Chem results, and therefore, the predicted aerosols highly depend on the performance of the GEOS-Chem model in simulating aerosol components, which is further linked to the aerosol emissions, MERRA-2 reanalysis data, and model parameterizations. The GEOS-Chem model has a relatively

low bias in simulating SO_4^{2-} globally (NMB<7%) but significantly overestimates NO_3^- and NH_4^+ over the U.S. (126 and 45%), Europe (127 and 90%), and Asia (269 and 167%).[63] The BC and OC concentrations are underestimated by the model over the U.S. (−7 and −20%), Europe (−25 and −49%), and China (−56 and −76%).[62,63] The bias of the GEOS-Chem model in simulating aerosols can also result in biases in aerosol prediction. This uncertainty can be reduced by training the model with observational data in future studies if more data are available over the entire globe.

Third, the biases can also arise from uncertainties in climate model results from CMIP6.[64,65] Moreover, the good performance of the trained RF model in 2010 does not guarantee a reliable extrapolation of model performance and results in response to a strong increase in temperature under future global warming. Besides, the RF model may overfit without setting a maximum depth of the tree, which requires additional work on the training data and machine learning model tuning in the future research. Last but not least, the machine learning model has relatively large biases in predicting OC and NO_3^- aerosols, especially over high-latitude regions, which need to be addressed in future studies by considering more aerosol processes and meteorological factors in the machine learning model.

◼ ASSOCIATED CONTENT

ⓈⒾ Supporting Information

The Supporting Information is available free of charge at https://pubs.acs.org/doi/10.1021/acs.est.1c04380.

> Additional descriptions and materials, including the machine learning method, comparison of results, model performance, variations in meteorological parameters, emissions, and predicted aerosol concentrations (PDF)

◼ AUTHOR INFORMATION

Corresponding Author

Yang Yang − *Jiangsu Key Laboratory of Atmospheric Environment Monitoring and Pollution Control, Jiangsu Collaborative Innovation Center of Atmospheric Environment and Equipment Technology, School of Environmental Science and Engineering, Nanjing University of Information Science and Technology, Nanjing 210044, China;* ⓞ orcid.org/0000-0002-9008-5137; Email: yang.yang@nuist.edu.cn

Authors

Huimin Li − *Jiangsu Key Laboratory of Atmospheric Environment Monitoring and Pollution Control, Jiangsu Collaborative Innovation Center of Atmospheric Environment and Equipment Technology, School of Environmental Science and Engineering, Nanjing University of Information Science and Technology, Nanjing 210044, China;* ⓞ orcid.org/0000-0001-8484-4566

Hailong Wang − *Atmospheric Sciences and Global Change Division, Pacific Northwest National Laboratory, Richland, Washington 99352, United States;* ⓞ orcid.org/0000-0002-1994-4402

Pinya Wang − *Jiangsu Key Laboratory of Atmospheric Environment Monitoring and Pollution Control, Jiangsu Collaborative Innovation Center of Atmospheric Environment and Equipment Technology, School of Environmental Science and Engineering, Nanjing University of Information Science and Technology, Nanjing 210044, China*

Xu Yue − *Jiangsu Key Laboratory of Atmospheric Environment Monitoring and Pollution Control, Jiangsu Collaborative Innovation Center of Atmospheric Environment and Equipment Technology, School of Environmental Science and Engineering, Nanjing University of Information Science and Technology, Nanjing 210044, China;* ⓞ orcid.org/0000-0002-8861-8192

Hong Liao − *Jiangsu Key Laboratory of Atmospheric Environment Monitoring and Pollution Control, Jiangsu Collaborative Innovation Center of Atmospheric Environment and Equipment Technology, School of Environmental Science and Engineering, Nanjing University of Information Science and Technology, Nanjing 210044, China*

Complete contact information is available at:
https://pubs.acs.org/10.1021/acs.est.1c04380

Notes

The authors declare no competing financial interest.

◼ ACKNOWLEDGMENTS

◼ REFERENCES

(1) Lelieveld, J.; Klingmüller, K.; Pozzer, A.; Burnett, R. T.; Haines, A.; Ramanathan, V. Effects of fossil fuel and total anthropogenic emission removal on public health and climate. *Proc. Natl. Acad. Sci. U.S.A.* **2019**, *116*, 7192−7197.

(2) IPCC. *Climate Change: The Physical Science Basis*; Cambridge University Press: Cambridge, U.K., 2013.

(3) Albrecht, B. A. Aerosols, cloud microphysics, and fractional cloudiness. *Science* **1989**, *245*, 1227−1230.

(4) Carslaw, K. S.; Lee, L. A.; Reddington, C. L.; Pringle, K. J.; Rap, A.; Forster, P. M.; Mann, G. W.; Spracklen, D. V.; Woodhouse, M. T.; Regayre, L. A.; Pierce, J. R. Large contribution of natural aerosols to uncertainty in indirect forcing. *Nature* **2013**, *503*, 67−71.

(5) Shindell, D.; Kuylenstierna, J. C. I.; Vignati, E.; van Dingenen, R.; Amann, M.; Klimont, Z.; Anenberg, S. C.; Muller, N.; Janssens-Maenhout, G.; Raes, F.; Schwartz, J.; Faluvegi, G.; Pozzoli, L.; Kupiainen, K.; Höglund-Isaksson, L.; Emberson, L.; Streets, D.; Ramanathan, V.; Hicks, K.; Oanh, N. T. K.; Milly, G.; Williams, M.; Demkine, V.; Fowler, D. Simultaneously mitigating near-term climate change and improving human health and food security. *Science* **2012**, *335*, 183−189.

(6) Yang, Y.; Wang, H.; Smith, S. J.; Zhang, R.; Lou, S.; Yu, H.; Li, C.; Rasch, P. J. Source apportionments of aerosols and their direct radiative forcing and long-term trends over continental United States. *Earth's Future* **2018**, *6*, 793−808.

(7) Yang, Y.; Lou, S.; Wang, H.; Wang, P.; Liao, H. Trends and source apportionment of aerosols in Europe during 1980−2018. *Atmos. Chem. Phys.* **2020**, *20*, 2579−2590.

(8) Streets, D. G.; Yu, C.; Wu, Y.; Chin, M.; Zhao, Z.; Hayasaka, T.; Shi, G. Aerosol trends over China, 1980−2000. *Atmos. Res.* **2008**, *88*, 174−182.

(9) Huang, J.; Pan, X.; Guo, X.; Li, G. Health impact of China's Air Pollution Prevention and Control Action Plan: an analysis of national air quality monitoring and mortality data. *Lancet Planet. Health* **2018**, *2*, e313−e323.

(10) Samset, B. H.; Lund, M. T.; Bollasina, M.; Myhre, G.; Wilcox, L. Emerging Asian aerosol patterns. *Nat. Geosci.* **2019**, *12*, 582−584.

(11) Malm, W. C.; Sisler, J. F.; Huffman, D.; Eldred, R. A.; Cahill, T. A. Spatial and seasonal trends in particle concentration and optical extinction in the United States. *J. Geophys. Res.* **1994**, *99*, 1347−1370.

(12) Tørseth, K.; Aas, W.; Breivik, K.; Fjæraa, A. M.; Fiebig, M.; Hjellbrekke, A. G.; Lund Myhre, C.; Solberg, S.; Yttri, K. E. Introduction to the European Monitoring and Evaluation Programme (EMEP) and observed atmospheric composition change during 1972−2009. *Atmos. Chem. Phys.* **2012**, *12*, 5447−5481.

(13) Chin, M.; Diehl, T.; Tan, Q.; Prospero, J. M.; Kahn, R. A.; Remer, L. A.; Yu, H.; Sayer, A. M.; Bian, H.; Geogdzhayev, I. V.; Holben, B. N.; Howell, S. G.; Huebert, B. J.; Hsu, N. C.; Kim, D.; Kucsera, T. L.; Levy, R. C.; Mishchenko, M. I.; Pan, X.; Quinn, P. K.; Schuster, G. L.; Streets, D. G.; Strode, S. A.; Torres, O.; Zhao, X.-P. Multi-decadal aerosol variations from 1980 to 2009: a perspective from observations and a global model. *Atmos. Chem. Phys.* **2014**, *14*, 3657−3690.

(14) Wang, Y.; Zhang, Q. Q.; He, K.; Zhang, Q.; Chai, L. Sulfate-nitrate-ammonium aerosols over China: response to 2000−2015 emission changes of sulfur dioxide, nitrogen oxides, and ammonia. *Atmos. Chem. Phys.* **2013**, *13*, 2635−2652.

(15) Li, H.; Yang, Y.; Wang, H.; Li, B.; Wang, P.; Li, J.; Liao, H. Constructing a spatiotemporally coherent long-term PM$_{2.5}$ concentration dataset over China using a machine learning approach. *Sci. Total Environ.* **2021**, *765*, 144263.

(16) Eyring, V.; Bony, S.; Meehl, G. A.; Senior, C. A.; Stevens, B.; Stouffer, R. J.; Taylor, K. E. Overview of the Coupled Model Intercomparison Project Phase 6 (CMIP6) experimental design and organization. *Geosci. Model Dev.* **2016**, *9*, 1937−1958.

(17) O'Neill, B. C.; Tebaldi, C.; van Vuuren, D. P.; Eyring, V.; Friedlingstein, P.; Hurtt, G.; Knutti, R.; Kriegler, E.; Lamarque, J.-F.; Lowe, J.; Meehl, G. A.; Moss, R.; Riahi, K.; Sanderson, B. M. The Scenario Model Intercomparison Project (ScenarioMIP) for CMIP6. *Geosci. Model Dev.* **2016**, *9*, 3461−3482.

(18) Collins, W. J.; Lamarque, J.-F.; Schulz, M.; Boucher, O.; Eyring, V.; Hegglin, M. I.; Maycock, A.; Myhre, G.; Prather, M.; Shindell, D.; Smith, S. J. AerChemMIP: quantifying the effects of chemistry and aerosols in CMIP6. *Geosci. Model Dev.* **2017**, *10*, 585−607.

(19) Thornhill, G. D.; Collins, W. J.; Kramer, R. J.; Olivié, D.; Skeie, R. B.; O'Connor, F. M.; Abraham, N. L.; Checa-Garcia, R.; Bauer, S. E.; Deushi, M.; Emmons, L. K.; Forster, P. M.; Horowitz, L. W.; Johnson, B.; Keeble, J.; Lamarque, J.-F.; Michou, M.; Mills, M. J.; Mulcahy, J. P.; Myhre, G.; Nabat, P.; Naik, V.; Oshima, N.; Schulz, M.; Smith, C. J.; Takemura, T.; Tilmes, S.; Wu, T.; Zeng, G.; Zhang, J. Effective radiative forcing from emissions of reactive gases and aerosols − a multi-model comparison. *Atmos. Chem. Phys.* **2021**, *21*, 853−874.

(20) Turnock, S. T.; Allen, R. J.; Andrews, M.; Bauer, S. E.; Deushi, M.; Emmons, L.; Good, P.; Horowitz, L.; John, J. G.; Michou, M.; Nabat, P.; Naik, V.; Neubauer, D.; O'Connor, F. M.; Olivié, D.; Oshima, N.; Schulz, M.; Sellar, A.; Shim, S.; Takemura, T.; Tilmes, S.; Tsigaridis, K.; Wu, T.; Zhang, J. Historical and future changes in air pollutants from CMIP6 models. *Atmos. Chem. Phys.* **2020**, *20*, 14547−14579.

(21) Zaveri, R. A.; Easter, R. C.; Singh, B.; Wang, H.; Lu, Z.; Tilmes, S.; Emmons, L. K.; Vitt, F.; Zhang, R.; Liu, X.; Ghan, S. J.; Rasch, P. J. Development and evaluation of chemistry-aerosol-climate model CAM5-chem-MAM7-MOSAIC: Global atmospheric distribution and radiative effects of nitrate aerosol. *J. Adv. Model. Earth Syst.* **2021**, *13*, No. e2020MS002346.

(22) Li, K.; Liao, H.; Zhu, J.; Moch, J. M. Implications of RCP emissions on future PM$_{2.5}$ air quality and direct radiative forcing over China. *J. Geophys. Res.: Atmos.* **2016**, *121*, 12985−13008.

(23) Lund, M. T.; Myhre, G.; Samset, B. H. Anthropogenic aerosol forcing under the Shared Socioeconomic Pathways. *Atmos. Chem. Phys.* **2019**, *19*, 13827−13839.

(24) Yang, Y.; Liao, H.; Lou, S. Increase in winter haze over eastern China in recent decades: Roles of variations in meteorological parameters and anthropogenic emissions. *J. Geophys. Res.: Atmos.* **2016**, *121*, 13,050−13,065.

(25) Cai, W.; Li, K.; Liao, H.; Wang, H.; Wu, L. Weather conditions conducive to Beijing severe haze more frequent under climate change. *Nat. Clim. Change* **2017**, *7*, 257−262.

(26) Hong, C.; Zhang, Q.; Zhang, Y.; Davis, S. J.; Tong, D.; Zheng, Y.; Liu, Z.; Guan, D.; He, K.; Schellnhuber, H. J. Impacts of climate change on future air quality and human health in China. *Proc. Natl. Acad. Sci. U.S.A.* **2019**, *116*, 17193−17200.

(27) Gonzalez-Abraham, R.; Chung, S. H.; Avise, J.; Lamb, B.; Salathé, E. P., Jr.; Nolte, C. G.; Loughlin, D.; Guenther, A.; Wiedinmyer, C.; Duhl, T.; Zhang, Y.; Streets, D. G. The effects of global change upon United States air quality. *Atmos. Chem. Phys.* **2015**, *15*, 12645−12665.

(28) Val Martin, M.; Heald, C. L.; Lamarque, J.-F.; Tilmes, S.; Emmons, L. K.; Schichtel, B. A. How emissions, climate, and land use change will impact mid-century air quality over the United States: a focus on effects at national parks. *Atmos. Chem. Phys.* **2015**, *15*, 2805−2823.

(29) Pendergrass, D. C.; Shen, L.; Jacob, D. J.; Mickley, L. J. Predicting the impact of climate change on severe wintertime particulate pollution events in Beijing using extreme value theory. *Geophys. Res. Lett.* **2019**, *46*, 1824−1830.

(30) Penrod, A.; Zhang, Y.; Wang, K.; Wu, S.-Y.; Leung, L. R. Impacts of future climate and emission changes on U.S. air quality. *Atmos. Environ.* **2014**, *89*, 533−547.

(31) Jacob, D. J.; Winner, D. A. Effect of climate change on air quality. *Atmos. Environ.* **2009**, *43*, 51−63.

(32) Gelaro, R.; McCarty, W.; Suárez, M. J.; Todling, R.; Molod, A.; Takacs, L.; Randles, C. A.; Darmenov, A.; Bosilovich, M. G.; Reichle, R.; Wargan, K.; Coy, L.; Cullather, R.; Draper, C.; Akella, S.; Buchard, V.; Conaty, A.; da Silva, A. M.; Gu, W.; Kim, G.-K.; Koster, R.; Lucchesi, R.; Merkova, D.; Nielsen, J. E.; Partyka, G.; Pawson, S.; Putman, W.; Rienecker, M.; Schubert, S. D.; Sienkiewicz, M.; Zhao, B. The Modern-Era Retrospective Analysis for Research and Applications, Version 2 (MERRA-2). *J. Clim.* **2017**, *30*, 5419−5454.

(33) Park, R. J.; Jacob, D. J.; Chin, M.; Martin, R. V. Sources of carbonaceous aerosols over the United States and implications for natural visibility. *J. Geophys. Res.: Atmos.* **2003**, *108*, 4355.

(34) Park, R. J.; Jacob, D. J.; Field, B. D.; Yantosca, R. M.; Chin, M. Natural and transboundary pollution influences on sulfate-nitrate-ammonium aerosols in the United States: Implications for policy. *J. Geophys. Res.: Atmos.* **2004**, *109*, D15204.

(35) Pye, H. O. T.; Liao, H.; Wu, S.; Mickley, L. J.; Jacob, D. J.; Henze, D. K.; Seinfeld, J. H. Effect of changes in climate and emissions on future sulfate-nitrate-ammonium aerosol levels in the United States. *J. Geophys. Res.: Atmos.* **2009**, *114*, D01205.

(36) Xu, X.; Wang, J.; Henze, D. K.; Qu, W.; Kopacz, M. Constraints on aerosol sources using GEOS-Chem adjoint and MODIS radiances, and evaluation with multisensor (OMI, MISR) data. *J. Geophys. Res.: Atmos.* **2013**, *118*, 6396−6413.

(37) Breider, T. J.; Mickley, L. J.; Jacob, D. J.; Wang, Q.; Fisher, J. A.; Chang, R. Y.-W.; Alexander, B. Annual distributions and sources of Arctic aerosol components, aerosol optical depth, and aerosol absorption. *J. Geophys. Res.: Atmos.* **2014**, *119*, 4107−4124.

(38) Li, S.; Zhang, L.; Cai, K.; Ge, W.; Zhang, X. Comparisons of the vertical distributions of aerosols in the CALIPSO and GEOS-Chem datasets in China. *Atmos. Environ. X* **2019**, *3*, 100036.

(39) Hoesly, R. M.; Smith, S. J.; Feng, L.; Klimont, Z.; Janssens-Maenhout, G.; Pitkanen, T.; Seibert, J. J.; Vu, L.; Andres, R. J.; Bolt, R. M.; Bond, T. C.; Dawidowski, L.; Kholod, N.; Kurokawa, J.-I.; Li, M.; Liu, L.; Lu, Z.; Moura, M. C. P.; O'Rourke, P. R.; Zhang, Q. Historical (1750−2014) anthropogenic emissions of reactive gases

and aerosols from the Community Emissions Data System (CEDS). *Geosci. Model Dev.* **2018**, *11*, 369−408.

(40) van der Werf, G. R.; Randerson, J. T.; Giglio, L.; van Leeuwen, T. T.; Chen, Y.; Rogers, B. M.; Mu, M.; van Marle, M. J. E.; Morton, D. C.; Collatz, G. J.; Yokelson, R. J.; Kasibhatla, P. S. Global fire emissions estimates during 1997−2016. *Earth Syst. Sci. Data* **2017**, *9*, 697−720.

(41) Zheng, B.; Tong, D.; Li, M.; Liu, F.; Hong, C.; Geng, G.; Li, H.; Li, X.; Peng, L.; Qi, J.; Yan, L.; Zhang, Y.; Zhao, H.; Zheng, Y.; He, K.; Zhang, Q. Trends in China's anthropogenic emissions since 2010 as the consequence of clean air actions. *Atmos. Chem. Phys.* **2018**, *18*, 14095−14111.

(42) Chen, Z.; Cai, J.; Gao, B.; Xu, B.; Dai, S.; He, B.; Xie, X. Detecting the causality influence of individual meteorological factors on local $PM_{2.5}$ concentration in the Jing-Jin-Ji region. *Sci. Rep.* **2017**, *7*, 40735.

(43) Chen, Z.; Xie, X.; Cai, J.; Chen, D.; Gao, B.; He, B.; Cheng, N.; Xu, B. Understanding meteorological influences on PM2.5 concentrations across China: a temporal and spatial perspective. *Atmos. Chem. Phys.* **2018**, *18*, 5343−5358.

(44) Di Virgilio, G.; Hart, M. A.; Jiang, N. Meteorological controls on atmospheric particulate pollution during hazard reduction burns. *Atmos. Chem. Phys.* **2018**, *18*, 6585−6599.

(45) El-Metwally, M.; Alfaro, S. C. Correlation between meteorological conditions and aerosol characteristics at an East Mediterranean coastal site. *Atmos. Res.* **2013**, *132−133*, 76−90.

(46) Freychet, N.; Tett, S. F. B.; Bollasina, M.; Wang, K. C.; Hegerl, G. C. The local aerosol emission effect on surface shortwave radiation and temperatures. *J. Adv. Model. Earth Syst.* **2019**, *11*, 806−817.

(47) Kaufman, Y. J.; Koren, I.; Remer, L. A.; Rosenfeld, D.; Rudich, Y. The Effect of Smoke, Dust, and Pollution Aerosol on Shallow Cloud Development over the Atlantic Ocean. *Proc. Natl. Acad. Sci. U.S.A.* **2005**, *102*, 11207−11212.

(48) Wang, D.; Jiang, B.; Lin, W.; Gu, F. Effects of aerosol-radiation feedback and topography during an air pollution event over the North China Plain during December 2017. *Atmos. Pollut. Res.* **2019**, *10*, 587−596.

(49) Yadav, R.; Beig, G.; Jaaffrey, S. N. A. The linkages of anthropogenic emissions and meteorology in the rapid increase of particulate matter at a foothill city in the Arawali range of India. *Atmos. Environ.* **2014**, *85*, 147−151.

(50) Yousefian, F.; Faridi, S.; Azimi, F.; Aghaei, M.; Shamsipour, M.; Yaghmaeian, K.; Hassanvand, M. S. Temporal variations of ambient air pollutants and meteorological influences on their concentrations in Tehran during 2012−2017. *Sci. Rep.* **2020**, *10*, 292.

(51) Stafoggia, M.; Bellander, T.; Bucci, S.; Davoli, M.; de Hoogh, K.; de'Donato, F.; Gariazzo, C.; Lyapustin, A.; Michelozzi, P.; Renzi, M.; Scortichini, M.; Shtein, A.; Viegi, G.; Kloog, I.; Schwartz, J. Estimation of daily PM_{10} and $PM_{2.5}$ concentrations in Italy, 2013−2015, using a spatiotemporal land-use random-forest model. *Environ. Int.* **2019**, *124*, 170−179.

(52) Wei, J.; Huang, W.; Li, Z.; Xue, W.; Peng, Y.; Sun, L.; Cribb, M. Estimating 1-km resolution $PM_{2.5}$ concentrations across China using the space-time random forest approach. *Remote Sens. Environ.* **2019**, *231*, 111221.

(53) Ren, L.; Yang, Y.; Wang, H.; Zhang, R.; Wang, P.; Liao, H. Source attribution of Arctic black carbon and sulfate aerosols and associated Arctic surface warming during 1980−2018. *Atmos. Chem. Phys.* **2020**, *20*, 9067−9085.

(54) Yang, Y.; Wang, H.; Smith, S. J.; Easter, R. C.; Rasch, P. J. Sulfate aerosol in the Arctic: Source attribution and radiative forcing. *J. Geophys. Res.: Atmos.* **2018**, *123*, 1899−1918.

(55) Liao, H.; Chen, W.-T.; Seinfeld, J. H. Role of climate change in global predictions of future tropospheric ozone and aerosols. *J. Geophys. Res.* **2006**, *111*, D12304.

(56) Hinks, M. L.; Montoya-Aguilera, J.; Ellison, L.; Lin, P.; Laskin, A.; Laskin, J.; Shiraiwa, M.; Dabdub, D.; Nizkorodov, S. A. Effect of relative humidity on the composition of secondary organic aerosol

from the oxidation of toluene. *Atmos. Chem. Phys.* **2018**, *18*, 1643−1652.

(57) Cheng, J.; Tong, D.; Zhang, Q.; Liu, Y.; Lei, Y.; Yan, G.; Yan, L.; Yu, S.; Cui, R. Y.; Clarke, L.; Geng, G.; Zheng, B.; Zhang, X.; Davis, S. J.; He, K. Pathways of China's $PM_{2.5}$ air quality 2015−2060 in the context of carbon neutrality. *Natl. Sci. Rev.* **2021**, *8*, nwab078.

(58) Cheng, J.; Tong, D.; Liu, Y.; Yu, S.; Yan, L.; Zheng, B.; Geng, G.; He, K.; Zhang, Q. Comparison of current and future $PM_{2.5}$ air quality in China under CMIP6 and DPEC emission scenarios. *Geophys. Res. Lett.* **2021**, *48*, No. e2021GL093197.

(59) Liu, S.; Xing, J.; Wang, S.; Ding, D.; Cui, Y.; Hao, J. Health Benefits of Emission Reduction under 1.5 °C Pathways Far Outweigh Climate-Related Variations in China. *Environ. Sci. Technol.* **2021**, *55*, 10957−10966.

(60) Liu, S.; Xing, J.; Zhang, H.; Ding, D.; Zhang, F.; Zhao, B.; Sahu, S. K.; Wang, S. Climate-driven trends of biogenic volatile organic compound emissions and their impacts on summertime ozone and secondary organic aerosol in China in the 2050s. *Atmos. Environ.* **2019**, *218*, 117020.

(61) Liu, S.; Xing, J.; Sahu, S. K.; Liu, X.; Liu, S.; Jiang, Y.; Zhang, H.; Li, S.; Ding, D.; Chang, X.; Wang, S. Wind-blown dust and its impacts on particulate matter pollution in Northern China: current and future scenarios. *Environ. Res. Lett.* **2021**, *16*, 114041.

(62) Luo, G.; Yu, F.; Moch, J. M. Further improvement of wet process treatments in GEOS-Chem v12.6.0: impact on global distributions of aerosols and aerosol precursors. *Geosci. Model Dev.* **2020**, *13*, 2879−2903.

(63) Fu, T.-M.; Cao, J. J.; Zhang, X. Y.; Lee, S. C.; Zhang, Q.; Han, Y. M.; Qu, W. J.; Han, Z.; Zhang, R.; Wang, Y. X.; Chen, D.; Henze, D. K. Carbonaceous aerosols in China: top-down constraints on primary sources and estimation of secondary contribution. *Atmos. Chem. Phys.* **2012**, *12*, 2725−2746.

(64) Kim, Y.-H.; Min, S. K.; Zhang, X.; Sillmann, J.; Sandstad, M. Evaluation of the CMIP6 multi-model ensemble for climate extreme indices. *Weather. Clim. Extremes* **2020**, *29*, 100269.

(65) Xu, Z.; Han, Y.; Tam, C.-Y.; Yang, Z.-L.; Fu, C. Bias-corrected CMIP6 global dataset for dynamical downscaling of the historical and future climate (1979−2100). *Sci. Data* **2021**, *8*, 293.